When the ground properties vary spatially, the bearing failure mechanism is no long symmetric and is attracted to weaker zones. Figure 4 shows what the failure mechanism might look like in a real soil. The lighter (weaker) region to the right of the footing attracts the failure mechanism, which is now non-symmetric. The failure mechanism is following the path of least resistance through the ground. What this means is that the traditionally assumed symmetric failure mechanism is unconservative -- it gives a higher strength than actually provided by the ground along its weakest path.

A natural approach to finding the weakest failure mechanism is to employ a finite element model of the ground (see, e.g., Smith and Griffiths, 2004). The basic idea is to simulate a random field of ground properties, map these properties to a finite element mesh and use the finite element method to predict the ground response. Figure 5 shows a cross-section through a finite element model of the ground under a stiff footing for a typical realization of the ground's effective elastic modulus field in a probabilistic settlement analysis.

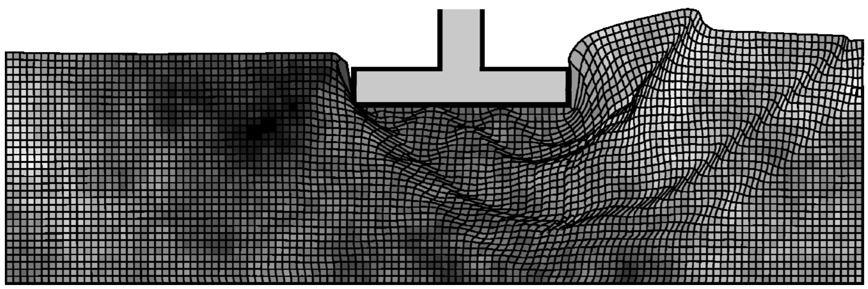

Fig. 4. Non-symmetric "weakest path" failure mechanism for spatially variable ground.

Some discussion of the relative merits of various methods of representing random fields in finite element analysis has been carried out over the years (see, for example, Li and Der Kiureghian, 1993). While using a spatially averaged discretization of the random field is just one approach to the problem, it is appealing in the sense that it reflects the simplest idea of the finite element representation of a continuum as well as the way that soil samples are typically taken and tested in practice, ie. as local averages. Regarding the discretization of random fields for use in finite element analysis, Matthies et al. (1997) makes the comment that "One way of making sure that the stochastic field has the required structure is to assume that it is a local averaging process.", referring to the conversion of a nondifferentiable to a differentiable (smooth) stochastic process. Matthie further goes on to say that the advantage of the local average representation of a random field is that it yields accurate results even for rather coarse meshes.

Following this reasoning, realizations of the ground property random field are produced using the Local Average Subdivision (LAS) method (Fenton and Vanmarcke, 1990). Specifically, LAS produces a discrete grid of local averages, $G_e\left(\underset{\sim}{x}_i\right)$, of a standard Gaussian random field, having correlation structure given by, for example, Eq. 2, where $\underset{\sim}{x}_i$ are the coordinates of the centroid of the *i*'th grid cell.

In detail, $G_e(\underset{\sim}{x}_i)$ is the local arithmetic average of a continuous standard Gaussian random field, $G(\underset{\sim}{x})$, over the element having centroid $\underset{\sim}{x}_i$.

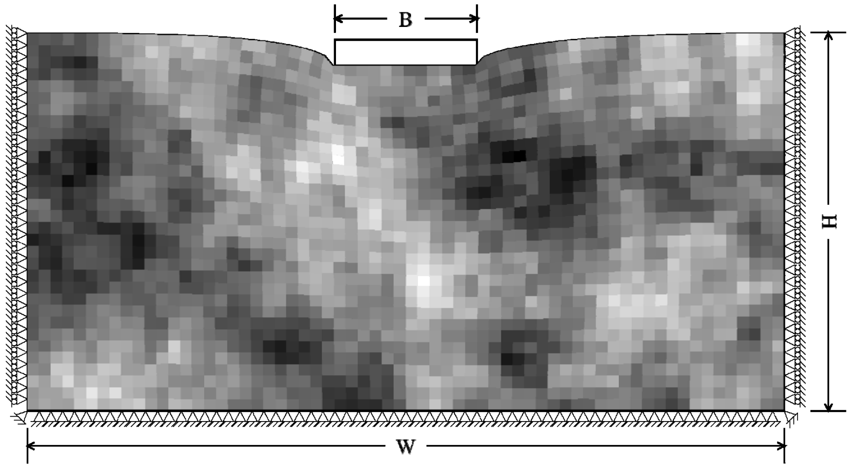

Fig. 5. Cross-section through a realization of the spatially random elastic modulus underlying a footing. Lighter soils are less stiff.

If the ground property in question is assumed to be lognormally distributed, as is commonly the case, these local averages are then mapped to finite element properties according to

$$X_e(\underset{\sim}{x}_i) = \exp\{\mu_{\ln X} + \sigma_{\ln X} G_e(\underset{\sim}{x}_i)\} \tag{7}$$

where X_e is the property assigned to the i'th finite element, $\mu_{\ln X}$ is the mean of $\ln X$, and $\sigma_{\ln X}$ is the *point* standard deviation of $\ln X$.

One of the features of using local arithmetic averaging is that the variance of the average reduces as the element size (averaging dimension) increases. Since a finite element generally employs low-order shape functions to approximate the behaviour of a continuum, the finite element is essentially modeling the average behaviour of the material within the domain of the element. Thus, it makes sense to use an average of the material properties within the element, which implies that the variance of the material property assigned to the element should reduce as the element becomes coarser (more averaging). In other words, the wedding of a local average random field with the (low-order shape function) finite element method is natural and consistent.

EFFECT OF SPATIAL VARIABILITY

To illustrate the effect that spatial variability has on the response of the ground to external or internal loads, two examples will be considered below.

Shallow Foundation Settlement

The RFEM can be used to estimate distribution of settlements of a single footing, as shown in Figure 5, and estimate the probability density function governing total settlement of the footing as a function of footing width for various statistics of the underlying soil. In this example, only the soil elasticity is considered to be spatially random. In addition, the soil is assumed to be isotropic – that is, the correlation structure is assumed to be the same in both the horizontal and vertical directions. Although soils generally exhibit a stronger correlation in the horizontal direction, due to their layered nature, the degree of anisotropy is site specific. In that this example is demonstrating the basic probabilistic behaviour of settlement, anisotropy is left as a refinement for the reader. The program used to perform the study presented in this example is RSETL2D (Fenton and Griffiths 2002, Griffiths and Fenton 2007; see also http://www.engmath.dal.ca/rfem).

Assuming that the settlement, δ of a single footing is lognormally distributed, as was found to be reasonable by Fenton and Griffiths (2002), having probability density function

$$f_\delta(x) = \frac{1}{\sqrt{2\pi}\sigma_{\ln\delta}x}\exp\left\{-\frac{1}{2}\left(\frac{\ln x - \mu_{\ln\delta}}{\sigma_{\ln\delta}}\right)^2\right\}, \qquad 0 \le x < \infty \tag{8}$$

the task is to estimate the parameters $\mu_{\ln\delta}$ and $\sigma_{\ln\delta}$ as functions of the footing width, B, elastic modulus standard deviation, σ_E, and correlation length $\theta_{\ln E}$. Figure 6 shows how the estimator of $\mu_{\ln\delta}$, denoted $m_{\ln\delta}$, varies with $\sigma^2_{\ln E}$ for $B = 0.1H$. All correlation lengths are drawn in the plot, but are not individually labeled since they lie so close together. This observation implies that the mean log-settlement is largely independent of the correlation length, $\theta_{\ln E}$. This is as expected since the correlation length does not affect the mean of a local average of a normally distributed process. Figure 6 suggests that the mean of log-settlement can be closely estimated by a straight line of the form,

$$\mu_{\ln\delta} = \ln(\delta_{det}) + \frac{1}{2}\sigma^2_{\ln E} \tag{9}$$

where δ_{det} is the `deterministic' settlement obtained from a single finite element analysis (or appropriate approximate calculation) of the problem using $E = \mu_E$ everywhere. This equation is also shown in Figure 6 and it can be seen that the agreement is very good. Even closer results were found for other footing widths.

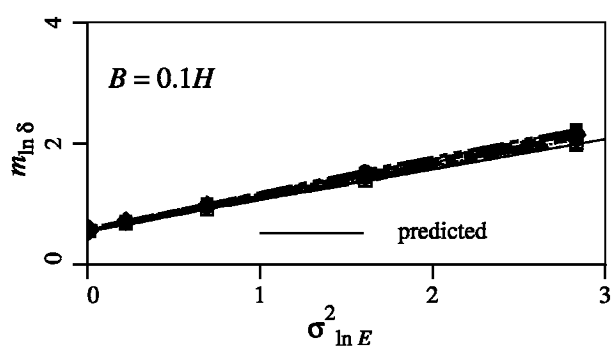

Fig. 6. Estimated mean of log-settlement along with that predicted by Eq. 9.

Estimates of the standard deviation of log-settlement, $s_{\ln\delta}$, are plotted in Figure 7 (as symbols) for two different footing widths. Intermediate footing widths give similar results. In all cases, $s_{\ln\delta}$ increases to $\sigma_{\ln E}$ as $\theta_{\ln E}$ increases. The reduction in variance as $\theta_{\ln E}$ decreases is due to the local averaging variance reduction of the log-elastic modulus field under the footing (for smaller $\theta_{\ln E}$, there are more 'independent' random field values, so that the variance reduces faster under averaging).

Following this reasoning, and assuming that local averaging of the area under the footing accounts for all of the variance reduction seen in Figure 7, the standard deviation of log-settlement is

$$\sigma_{\ln\delta} = \sqrt{\gamma(B,H)}\,\sigma_{\ln E} \tag{10}$$

where $\gamma(B,H)$ is the variance reduction function, which depends on the averaging region, $B \times H$ as well as on the correlation length, $\theta_{\ln E}$. Since $\sigma_{\ln E}$ is constant for each value of σ_E / μ_E, Figure 7 is essentially a plot of the variance function, $\gamma(B,H)$, illustrating how the variance of a local average decreases as the correlation length decreases. Predictions of $\sigma_{\ln\delta}$ using Eq. 10 are superimposed on Figure 7 using lines. The agreement is remarkable.

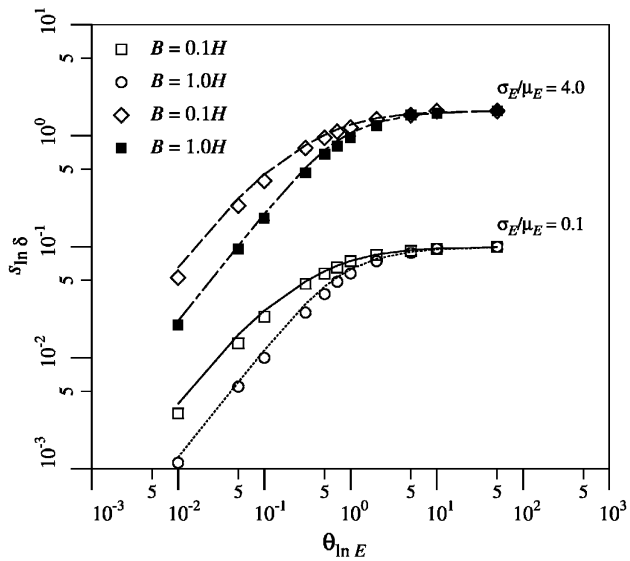

Fig. 7. Comparison of simulated sample standard deviation of log-settlement, shown with symbols, with theoretical estimate via Eq. 10, shown with lines.

An alternative physical interpretation of Eq's 9 and 10 comes by generalizing the settlement prediction to the form

$$\delta = \frac{\delta_{det}\mu_E}{E_g} \tag{11}$$

where E_g is the geometric average of the elastic modulus values over the region of influence,

$$E_g = \exp\left\{\frac{1}{BH}\int_0^H \int_0^B \ln E(x,y)\,dx\,dy\right\} \tag{12}$$

Taking the logarithm of Eq. 11 and then computing its mean and variance leads to Eq's 9 and 10. The geometric mean is dominated by small values of elastic modulus, which means that the total settlement is dominated by low elastic modulus regions underlying the footing, as would be expected.

These results can be extended to the serviceability limit state design of a single footing. If a square footing of dimension $B \times B$ is considered, the design requirement is to find B and the ratio of the load to resistance factors, α / φ_g, such that

$$\delta_{max} = u_1 \left(\frac{\alpha \hat{F}}{B \varphi_g \hat{E}} \right) \tag{13}$$

and

$$\mathrm{P}\left[u_1 \ \frac{F}{BE_{eff}} > u_1 \left(\frac{\alpha \hat{F}}{B \varphi_g \hat{E}} \right) \right] = p_m \tag{14}$$

where δ_{max} is the maximum tolerable settlement (serviceability limit state), u_1 is an influence factor (see Fenton et al., 2005, for more details), F is the actual load, E_{eff} is the equivalent elastic modulus as seen by the footing, $\hat{F}$ is the characteristic (nominal) load, $\hat{E}$ is the characteristic (nominal) elastic modulus, and p_m is the maximum tolerable failure probability. In the above, we are assuming that the soil's elastic modulus is the 'resistance' to the load and that it is to be factored due to its high uncertainty.

Five different sampling schemes will be considered in this example, as illustrated in Figure 8. The outer solid line denotes the edge of the soil model, which is 9.6 x 9.6 m in plan and 4.8 m in depth as in Figure 5, and the interior dashed line the location of the footing. The small black squares show the plan locations where the site is virtually sampled. It is expected that the quality of the estimate of E_{eff} will improve for higher numbered sampling schemes. That is, the probability of design failure will decrease for higher numbered sampling schemes, everything else being held constant.

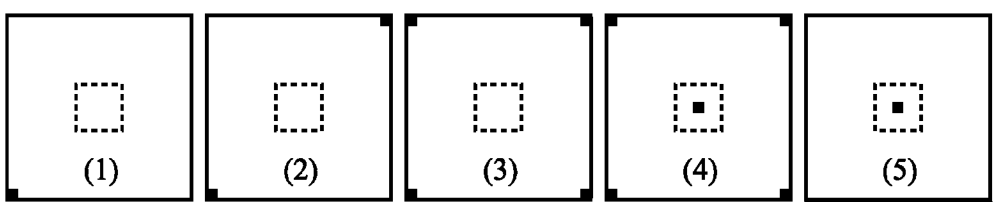

Fig. 8. Sampling schemes considered in this example.

For fixed resistance factor, φ_g, the soil samples allow an estimate of the characteristic elastic modulus, $\hat{E}$ and Eq. 13 can then be used to design the footing. Repeating the design for many realizations of the soil allows the probability that a footing design using φ_g will result in excessive settlement to be estimated. Figure 9 illustrates the effect of correlation length on the probability of excessive settlement, p_f, for sampling scheme #1. It is evident that a) spatial variability of the ground has a strong influence on p_f, and b) that there is a worst case correlation length, in this case around 10 m – which is of the order of the distance from the footing to the sampling point (6.8 m).

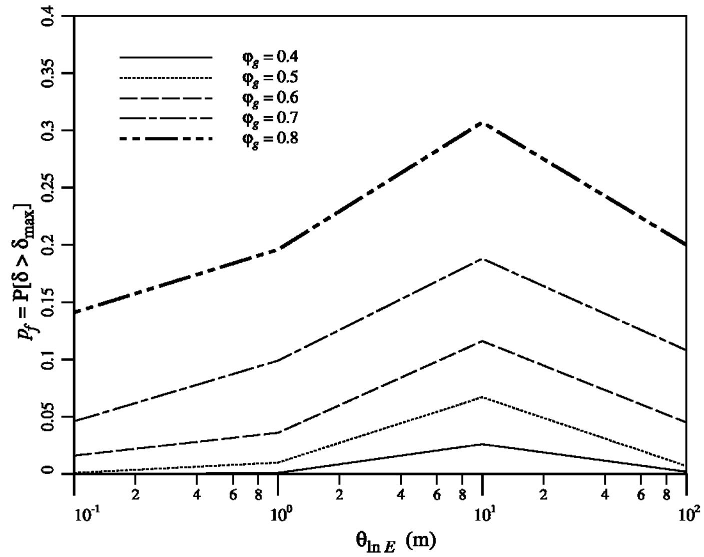

Fig. 9. Effect of correlation length $\theta_{\ln E}$ on probability of excessive settlement $p_f = P[\delta > \delta_{max}]$.

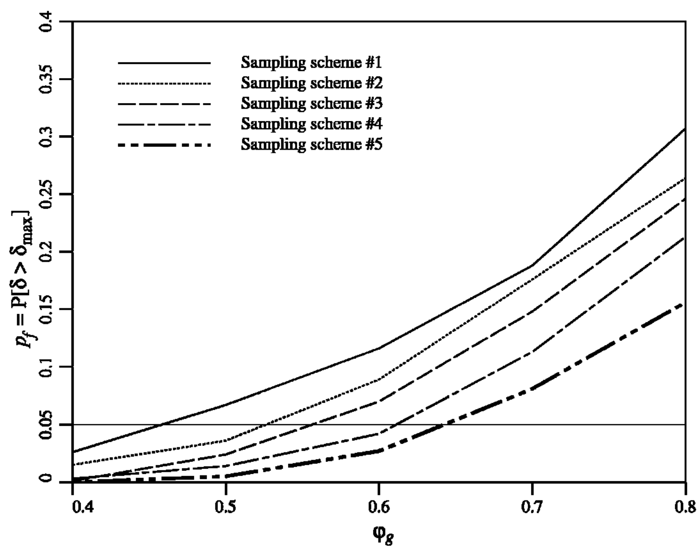

Fig. 10. Effect of resistance factor φ_g on probability of failure $p_f = P[\delta > \delta_{max}]$ for $v_E = 0.5$ and $\theta_{\ln E} = 10$ m.

Figure 10 shows the failure probability for the various sampling schemes at a coefficient of variation, $v_E = 0.5$, and $\theta_{\ln E} = 10$ m. Improved sampling (i.e. improved understanding of the site) makes a significant difference to the required value of φ_g, which ranges from $\varphi_g \approx 0.46$ for sampling scheme #1 to $\varphi_g \approx 0.65$ for sampling scheme #5, assuming a target probability of $p_m = 0.05$. Note that if a distance-weighted or trend estimate were used, sampling scheme #4 would have been better than #5. In general, more samples are preferable – however, only a simple average was used in this study to estimate the soil properties so that the four samples not taken directly under the footing in sampling scheme #4 actually just "muddy the waters", decreasing the accuracy of the sample taken under the footing. The overall implications of Figure 10 are that when soil variability is significant, considerable design/construction savings can be achieved when the sampling scheme is improved.

Bearing Capacity

The design of a shallow footing typically begins with a site investigation aimed at determining the strength of the founding soil or rock. Once this information has been gathered, the geotechnical engineer is in a position to determine the footing dimensions required to avoid entering various limit states. In so doing, it will be assumed here that the geotechnical engineer is in close communication with the structural engineer(s) and is aware of the loads that the footings are being designed to support. The limit states that are usually considered in the footing design are serviceability limit states (typically deformation – see example above) and ultimate limit states. The latter is concerned with safety and includes the load-carrying capacity, or *bearing capacity*, of the footing.

This example illustrates an LRFD approach for shallow foundations designed against bearing capacity failure. The design goal is to determine the footing dimensions such that the *ultimate geotechnical resistance* based on characteristic soil properties, $\hat{R}_u$, satisfies

$$\varphi_g \hat{R}_u \geq \sum_i \alpha_i \hat{F}_i \tag{15}$$

where φ_g is the *geotechnical resistance factor*, α_i is the *i*'th *load factor*, and $\hat{F}_i$ is the *i*'th *characteristic load effect*. The relationship between φ_g and the probability that the designed footing will experience a bearing capacity failure will be summarized below (from Fenton et al., 2007) followed by some results on resistance factors required to achieve certain target maximum acceptable failure probabilities for the particular case of a strip footing (from Fenton et al., 2008).

The characteristic ultimate geotechnical resistance $\hat{R}_u$ is determined using characteristic soil properties, in this case characteristic values of the soil's cohesion, *c*, and friction angle, ϕ (note that although the primes are omitted from these quantities it should be recognized that the theoretical developments described in this example are applicable to either total or effective strength parameters).

The characteristic value of the cohesion, $\hat{c}$, is defined here as the median of the sampled observations, c_i^o, which, assuming *c* is lognormally distributed, can be computed using the geometric average,

$$\hat{c} = \left[\prod_{i=1}^{m} c_i^o\right]^{1/m} = \exp\left\{\frac{1}{m}\sum_{i=1}^{m} \ln c_i^o\right\} \tag{16}$$

The geometric average is used here because if *c* is lognormally distributed, as assumed, then $\hat{c}$ will also be lognormally distributed. The characteristic value of the friction angle is computed as an arithmetic average

$$\hat{\phi} = \frac{1}{m}\sum_{i=1}^{m} \phi_i^o \tag{17}$$

The arithmetic average is used here because ϕ is assumed to follow a symmetric bounded distribution and the arithmetic average preserves the mean. That is, the mean of $\hat{\phi}$ is the same as the mean of ϕ.

To determine the characteristic ultimate geotechnical resistance $\hat{R}_u$, it will first be assumed that the soil is weightless (and thus cohesive). This simplifies the calculation of the ultimate bearing stress q_u to

$$q_u = c\, N_c \tag{18}$$

The assumption of weightlessness is conservative since the soil weight contributes to the overall bearing capacity. This assumption also allows the analysis to explicitly concentrate on the role of $c\, N_c$ on ultimate bearing capacity, since this is the only term that includes the effects of spatial variability relating to *both* shear strength parameters c and ϕ.

Bearing capacity predictions, involving specification of the N_c factor in this case, are generally based on plasticity theories (see, e.g., Prandtl, 1921; Terzaghi, 1943; and Sokolovski, 1965) in which a rigid base is punched into a softer material. These theories assume that the soil underlying the footing has properties which are spatially constant (everywhere the same). This type of ideal soil will be referred to as a *uniform soil* henceforth. Under this assumption, most bearing capacity theories (e.g., Prandtl, 1921; Meyerhof, 1951, 1963) assume that the failure slip surface takes on a logarithmic spiral shape to give

$$N_c = \frac{e^{\pi \tan\phi} \tan^2\left(\frac{\pi}{4} + \frac{\phi}{2}\right) - 1}{\tan\phi} \tag{19}$$

The theory is derived for the general case of a $c-\phi$ soil. One can always set $\phi = 0$ to obtain results for an undrained clay.

Consistent with the theoretical results presented by Fenton et al. (2008), this example will concentrate on the design of a strip footing. In this case, the characteristic ultimate geotechnical resistance $\hat{R}_u$ becomes

$$\hat{R}_u = B\hat{q}_u \tag{20}$$

where B is the footing width and $\hat{R}_u$ has units of load per unit length out-of-plane, that is, in the direction of the strip footing. The characteristic ultimate bearing stress $\hat{q}_u$ is defined by

$$\hat{q}_u = \hat{c}\hat{N}_c \tag{21}$$

where the characteristic N_c factor is determined using the characteristic friction angle in Eq. 19,

$$\hat{N}_c = \frac{e^{\pi \tan\hat{\phi}} \tan^2\left(\frac{\pi}{4} + \frac{\hat{\phi}}{2}\right) - 1}{\tan\hat{\phi}} \tag{22}$$

For the strip footing and just the dead and live load combination, the LRFD equation becomes

$$\varphi_g B\hat{q}_u = \left[\alpha_L \hat{F}_L + \alpha_D \hat{F}_D\right] \quad \Rightarrow \quad B = \frac{\left[\alpha_L \hat{F}_L + \alpha_D \hat{F}_D\right]}{\varphi_g \hat{q}_u} \qquad (23)$$

To determine the resistance factor φ_g required to achieve a certain acceptable reliability of the constructed footing, it is necessary to estimate the probability of bearing capacity failure of a footing designed using Eq. 23. Once the probability of failure p_f for a certain design using a specific value for φ_g is known, this probability can be compared to the maximum acceptable failure probability p_m . If p_f exceeds p_m, then the resistance factor must be reduced and the footing redesigned. Similarly, if p_f is less than p_m, then the design is overconservative and the value of φ_g can be increased. Using either simulation or theory, design curves can then be developed from which the value of φ_g required to achieve a maximum acceptable failure probability can be determined.

Figure 11 shows the resistance factors required for the case where the soil is sampled at a distance of $r = 4.5$ m from the footing centerline for the target failure probability, $p_m = 0.001$. In the figure, v_c is the coefficient of variation of cohesion.

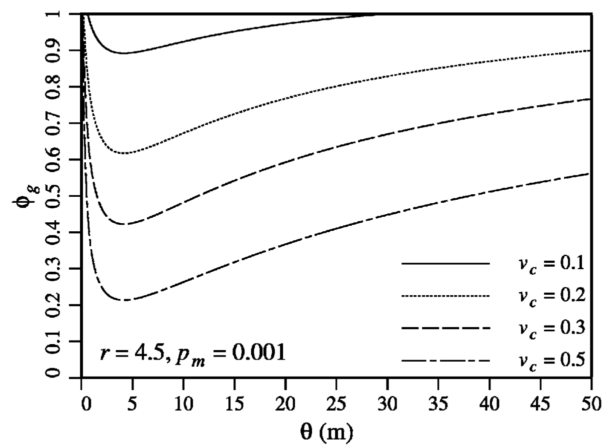

Fig. 11. Resistance factors required to achieve acceptable failure probability p_m when soil is sampled at $r = 4.5$ m from footing centerline and $p_m = 0.001$.

The worst-case correlation length is evidently about 5 m. This worst-case correlation length is of the same magnitude as the mean footing width which can be explained as follows: If the random soil fields are stationary, then soil samples yield perfect information, regardless of their location, if the correlation length is either zero (assuming soil sampling involves some local averaging) or infinity. When the information is perfect, the probability of a bearing capacity failure goes to zero and $\varphi_g \rightarrow 1.0$ (or possibly greater than 1.0 to compensate for the load bias factors). When the correlation length is zero, the soil sample will consist of an infinite number of independent "observations" whose average is equal to the true mean (or true median, if the average is a geometric average). Since the footing also averages the soil properties, the footing 'sees' the same true mean (or true median) value predicted by the soil sample. When the correlation length goes to infinity, the soil becomes uniform, having the same value everywhere. In this case, any soil sample also perfectly predicts conditions under the footing.

At intermediate correlation lengths soil samples become imperfect estimators of conditions under the footing, and so the probability of bearing capacity failure increases, or equivalently, the required resistance factor decreases. Thus, the minimum required resistance factor will occur at some correlation length between 0 and infinity. The precise value depends on the geometric characteristics of the problem under consideration, such as the footing width, depth to bedrock, length of soil sample, and/or the distance to the sample point.

RELIABILITY-BASED GEOTECHNICAL DESIGN CODE DEVELOPMENT

A report by Littlejohn (1991) entitled *Inadequate Site Investigation* made the statement "You pay for a site investigation whether you have one or not", which quite clearly points out the cost of geotechnical uncertainty. Essentially, if one does not bother with a sufficient geotechnical investigation, one either pays the cost immediately by requiring a more conservative design or is going to pay the cost later due to some level of performance failure of the designed system. Since performance failure at some future date is generally very expensive, there is a real desire in the geotechnical community to account for the level of uncertainty during the design phase. That is, the level of site and modeling understanding should be balanced against the conservatism of the design – the greater the understanding, the less conservative, and thus less expensive, the design. Site understanding refers to how well the ground providing the geotechnical resistance is known and model understanding means the degree of confidence that a designer has in the (usually mathematical) model used to predict the geotechnical resistance.

To provide for designs that account for degree of understanding, it makes sense to have a resistance factor which is adjusted as a function of site and model understanding. There are at least two advantages to such an approach: 1) overall safety can be maintained at a common target maximum failure probability, and 2) the direct economic advantage related to increasing site and model understanding can be demonstrated. For example, the pre-2014 Canadian design codes specify a single resistance factor for bearing capacity design (0.5). It doesn't matter how confident one is in one's prediction of the bearing capacity of a foundation, the same resistance factor must be used. Thus, there is no direct advantage to improving the geotechnical response prediction. If only a single resistance factor can be used, one might as well spend the least amount of time one can on the site investigation and modeling.

The resulting desire for a resistance factor which depends on site and model understanding is not new. The Australian Standard for *Bridge Design, Part 3: Foundations and Soil-Supporting Structures* (AS 5100.3, Standards Australia, 2004) provides a range in "geotechnical strength reduction factors" accompanied by guidance as to which end of the scale should be used. For example, AS 5100.3 suggests that the lower end of the resistance factor range (more conservative) should be used for limited site investigations, simple methods of calculation, severe failure consequences, and so on. It is of interest to note that the Australian Standard